JOURNAL OF GEOPHYSICAL RESEARCH, VOL. 114, A00F02, doi:10.1029/2009JA014366, 2009

Oblique lower band chorus waves: Time shifts between discrete elements observed by the Cluster spacecraft

Jaroslav Chum,[1] Ondrej Santolik,[2,3] Donald A. Gurnett,[4] and Jolene S. Pickett[4]

Received 16 April 2009; revised 16 July 2009; accepted 15 September 2009; published 15 December 2009.

[1] We report observations of remarkable frequency differences and time shifts between the corresponding elements of lower band chorus recorded by the four Cluster spacecraft at low magnetic latitudes on 20 January 2004. The Poynting flux measurements made by the Spatio-Temporal Analysis of Field Fluctuations (STAFF) instrument confirm that the chorus source is located in the magnetic equatorial plane. Surprisingly, the spacecraft located closer to the equator systematically received the corresponding chorus elements later than the spacecraft located at higher magnetic latitudes. Owing to the orbit, the spacecraft located closer to the equator were at lower L shells. The time shifts and frequency differences depended almost linearly on the perpendicular distance between the various spacecraft. Analysis of data from both the wideband data and STAFF instruments shows that chorus emissions were generated with highly oblique angles of propagation. We discuss several properties of the chorus source that could lead to these observations. We show that the sources moving across the magnetic field lines are reasonably consistent with these observations. We propose that the transverse motion of the chorus sources is a consequence of a feedback between the oblique waves and counter streaming electrons during nonlinear cyclotron interactions, and we provide an estimate of the transverse velocity of the source.

Citation: Chum, J., O. Santolik, D. A. Gurnett, and J. S. Pickett (2009), Oblique lower band chorus waves: Time shifts between discrete elements observed by the Cluster spacecraft, *J. Geophys. Res.*, *114*, A00F02, doi:10.1029/2009JA014366.

1. Introduction

[2] Chorus waves are relatively intense electromagnetic emissions generated close to the magnetic equatorial plane at radial distances from ~3 to ~10 Earth radii *Re* [*Santolik et al.*, 2005b], and are characterized by discrete features in frequency-time spectrograms. Chorus usually consists of tones rising in frequency at a rate from ~0.1 to ~10 kHz/s. Less frequently, falling tones are observed. The frequency of chorus is controlled by the equatorial cyclotron frequency f_{ceq}. At the equator, chorus often occurs in two frequency bands separated by a narrow gap at 0.5 f_{ceq}. The lower band is observed in the range of ~0.1 to ~0.45 f_{ceq}, and the upper band at ~0.5 to ~0.7 f_{ceq} [*Burtis and Helliwell*, 1976; *Sazhin and Hayakawa*, 1992]. Chorus has also been observed in the magnetospheres of Jupiter [*Gurnett and Scarf*, 1981; *Menietti et al.*, 2008] and Saturn [*Reinleitner et al.*, 1984].

[3] The exact mechanism of chorus generation is still a subject of investigation. It is generally accepted that chorus is generated by a nonlinear process based on the electron cyclotron resonance of whistler mode waves with energetic electrons [*Omura et al.*, 1991; *Nunn et al.*, 1997; *LeDocq et al.*, 1998]. *Trakhtengerts* [1995, 1999] introduced a theory of the backward wave oscillator to explain the discrete features of chorus and the formation of the chorus frequency spectrum [*Trakhtengerts et al.*, 2007]. *Omura and Summers* [2006] found that some of the resonating electrons are depleted in phase space. This gives rise to a resonant current which is responsible for the growth of the wave amplitude [*Omura et al.*, 2008]. *Omura et al.* [2008] also showed that for nonlinear wave growth either a frequency variation or a spatial inhomogeneity of the static magnetic field is necessary. The wave amplitude is amplified by the nonlinear resonant current, which is sustained by the increasing inhomogeneity of the dipole magnetic field over some distance from the equator. *Omura et al.* [2008] found that chorus elements are generated successively at the equator so long as a sufficient flux of energetic electrons with a strong temperature anisotropy is present. The topic of chorus waves draws attention because of the potential for chorus to accelerate electrons to relativistic energies [e.g., *Horne and Thorne*, 2003; *Horne et al.*, 2005; *Omura and Summers*, 2006].

[4] The Poynting flux measurements on the Polar [*LeDocq et al.*, 1998] and Cluster satellites [*Santolik et al.*, 2004a, 2005a] showed that the chorus source is located close

[1]Department of Upper Atmosphere, Institute of Atmospheric Physics, Prague, Czech Republic.
[2]Department of Space Physics, Institute of Atmospheric Physics, Prague, Czech Republic.
[3]Faculty of Mathematics and Physics, Charles University, Prague, Czech Republic.
[4]Department of Physics and Astronomy, University of Iowa, Iowa City, Iowa, USA.

0148-0227/09/2009JA014366$09.00

to the geomagnetic equatorial plane with the typical dimension along the magnetic field line being ~3000 to ~5000 km. The cross correlation of spectrograms containing lower band chorus recorded on different Cluster spacecraft provided an estimate of the transverse dimension (with respect to the magnetic field) of the chorus source. The cross-correlation coefficients rapidly decreased at distances larger than 100 km [*Santolik and Gurnett*, 2003].

[5] The multipoint observations of the Cluster spacecraft revealed another interesting phenomenon: frequency differences and time shifts have sometimes been observed between corresponding upper band chorus elements on different Cluster spacecraft [*Gurnett et al.*, 2001; *Inan et al.*, 2004; *Platino et al.*, 2006; *Breneman et al.*, 2007; *Chum et al.*, 2007]. In this paper, we analyze observations of remarkable time shifts and frequency differences between corresponding elements observed in the lower band chorus on 20 January 2004 when the Cluster spacecraft were approaching the magnetic equator from magnetic latitudes of ~15°. Section 2 presents the observations of chorus emissions by the wideband data (WBD) instruments [*Gurnett et al.*, 1997], and the results of wave normal analysis based on the multicomponent measurements made by the Spatio-Temporal Analysis of Field Fluctuations (STAFF) instruments [*Cornilleau-Wehrlin et al.*, 1997]. Section 3 reports the results of the cross-correlation analysis of individual records on different spacecraft. In section 4, we discuss possible properties of chorus sources that could lead to the observed time shifts and frequency differences. Section 5 summarizes our main results and conclusions.

2. Observations

[6] The best opportunities to record corresponding chorus elements on different spacecraft are when the spacecraft are separated at relatively small distances, less than ~1000 km. In our search for unusually large time shifts between the corresponding chorus elements on different spacecraft, we have limited our search to the lower band chorus occurring below 4 kHz in order to have simultaneous WBD records with high time resolution and multicomponent measurements of STAFF. We have also systematically limited ourselves to the events lasting several minutes. We have found two distinct events meeting these requirements. The first occurred on 6 January 2004 and lasted from 1237 to 1241 UT. The second event, recorded on 20 January 2004, lasted a longer time, approximately from 19:10 to 19:38 UT, the time interval being limited in this case by the operation time of the WBD instruments.

[7] Figure 1 presents power spectral intensities of one electric component observed by the WBD instrument on each of the four Cluster spacecraft during their approach to the equator on 20 January 2004 from 1910–1938 UT. The WBD instrument on spacecraft 3 was switched off at 1920 UT. The frequencies of the emissions increased as the satellites approached the equator; this is a consequence of the orbit having its perigee close to the equator. The geomagnetic activity was moderate, with Dst ~ −40 nT and Kp ~ 4.

[8] The expanded spectrograms in Figure 2 contain corresponding chorus elements with remarkable frequency differences and time shifts between the different spacecraft. Despite a relatively intense noise background, we can recognize that the discrete elements are falling tones. We note that falling tones were also observed in the cases containing significant time shifts of upper band chorus elements [*Platino et al.*, 2006; *Chum et al.*, 2007]. Referring to Figure 2 it is worth mentioning that the corresponding elements are received later on the spacecraft located closer to the geomagnetic equator, than on the spacecraft located at higher magnetic latitudes. It is necessary to note that the spacecraft located closer to the equator are also on lower L shells, and record waves of higher frequencies than the spacecraft located on higher L shells. The magnetic orbital positions of the Cluster spacecraft during the analyzed time interval are given in Figure 3. The Cluster spacecraft are color coded (SC1 is black, SC2 is red, SC3 is green, and SC4 is blue). Figures 3a and 3b show the *L* value and magnetic latitude *mlat* on the vertical axes versus time in seconds on the horizontal axes. Figure 3c represents the magnetic local time *mlt*. Figure 3d shows the measured electron cyclotron frequency f_{ce} (solid line), and the equatorial cyclotron frequency f_{ceq} along the field line (dashed line) calculated using the dipole field model.

[9] The simultaneous multicomponent measurements made by the STAFF instruments [*Cornilleau-Wehrlin et al.*, 1997] make it possible to calculate the wave normal angles of the observed waves. Analysis of these angles measured in the source region is given in the companion paper [*Santolik et al.*, 2009]. Figure 4 shows the wave normal angles in the selected time intervals in which we observed discrete chorus emissions as a function of time along the spacecraft orbit. The results were obtained by carrying out the plane wave analysis using the SVD method [*Santolik et al.*, 2003]. The polar wave normal angles θ were ~55–60° on all the spacecraft when they were approaching the magnetic equatorial plane at the end of the analysis interval, and were approximately 70–80° when the spacecraft were located at higher magnetic latitudes at the beginning of the analysis interval. These values suggest that the waves propagate at highly oblique angles, close to the resonance cone. See, e.g., *Lauben et al.* [2002], *Chum and Santolik* [2005], and *Bortnik et al.* [2007] for the recent ray-tracing studies of propagation of oblique chorus waves in the Earth's magnetosphere. The azimuthal angles φ were prevailingly close to zero, which means that the wave vectors were directed from the Earth. A certain spread in the measured values of wave normal angles suggests that chorus waves were probably generated with a span of wave normal angles, especially in the azimuthal angle φ. However, we do not observe significant differences between the values of wave normal angles observed on different spacecraft at the same time.

[10] The analysis of the Poynting flux confirms that the sources were located close to the geomagnetic equator. *Santolik et al.* [2009], in the companion paper, show that the chorus waves propagated southward at magnetic latitudes less than ~−2°.

3. Cross-Correlation Analysis

[11] We will proceed with the analysis of characteristic frequencies observed along spacecraft trajectories and with the analysis of the time shifts between the corresponding elements on different spacecraft. We perform the analysis in

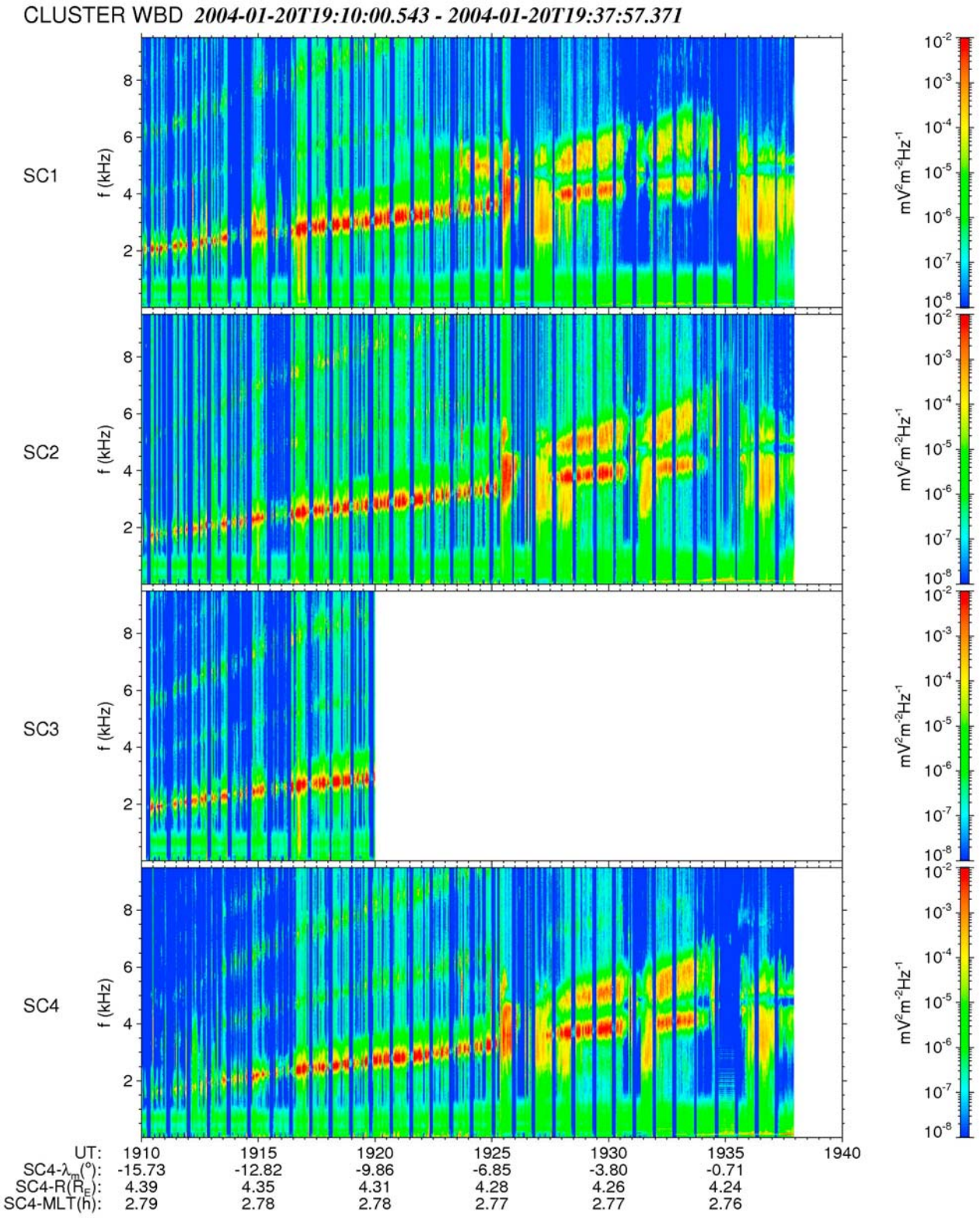

Figure 1. Overview spectrograms of the electric component of the wave field measured by the WBD instrument on different Cluster spacecraft from 1910 to 1940 on 20 January 2004. Orbital characteristics are related to SC4. The blue vertical lines correspond to time intervals in which the magnetic antennas are sampled.

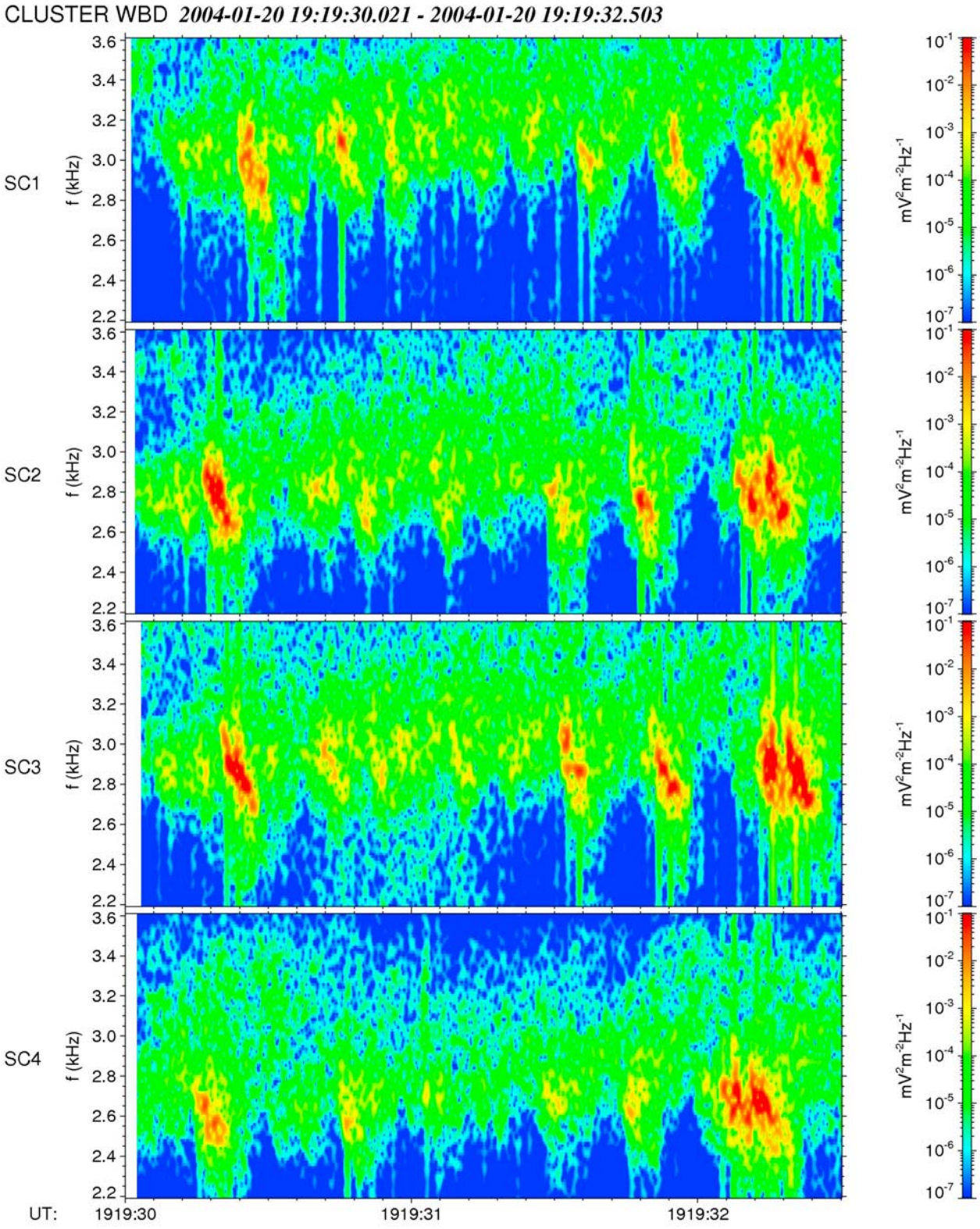

Figure 2. Detailed spectrograms recorded between 1919:30 and 1919:32.5 UT showing the frequency differences and time shifts between the corresponding elements when observed on different spacecraft.

selected time intervals in which we clearly observed the chorus elements. We note that a noise band, as opposed to discrete emissions, was observed at some of these times. We calculate characteristic frequencies f as arithmetic means of frequencies at which spectral intensities of chorus elements fall to one quarter of their maximum values.

[12] In order to obtain the time shifts between the corresponding elements, we selected several short time

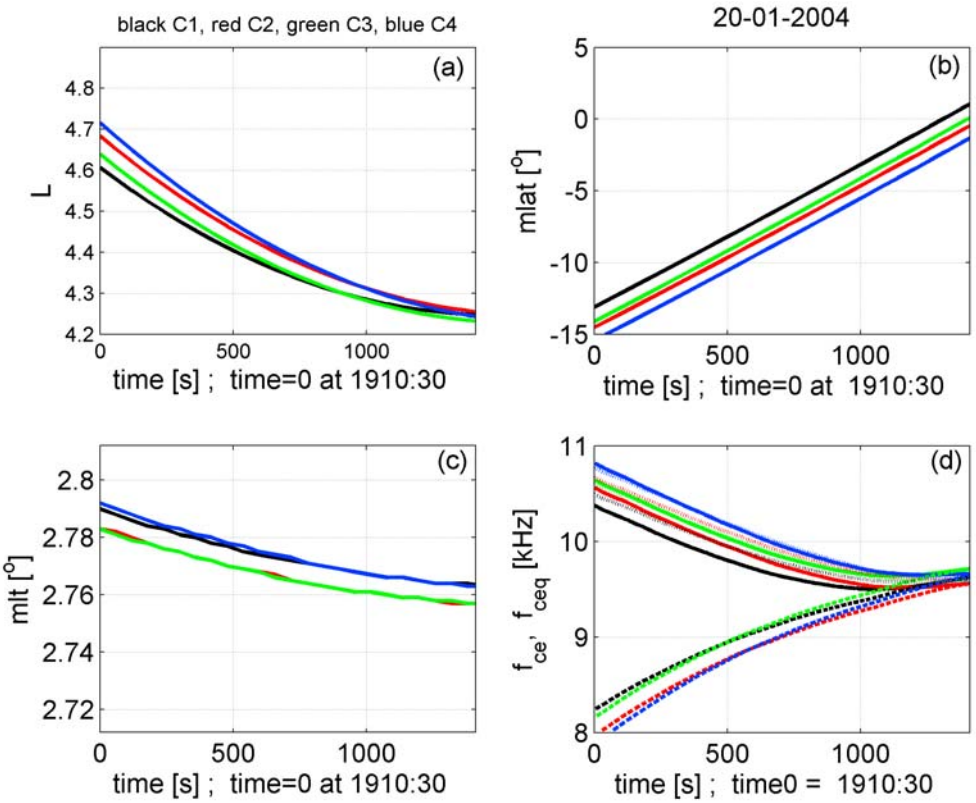

Figure 3. Magnetic orbital characteristics of different Cluster spacecraft as functions of time during the analyzed time interval. The reference start time is 1910:30 UT on 20 January 2004. The Cluster spacecraft are color coded as follows: SC1 is black, SC2 is red, SC3 is green, and SC4 is blue. (a) L shell, and (b) magnetic latitude *mlat*. (c) Magnetic local time *mlt*. (d) Measured cyclotron frequencies f_{ce} along the orbit (solid lines), the equatorial cyclotron frequencies f_{ceq} (dashed lines) calculated from f_{ce} while using the dipole magnetic field model, and the $f_{ceq(4.25)}$ frequencies (dotted lines). See the text for more details.

intervals (from ~5 to ~10s) containing lower band chorus emissions with corresponding elements observed simultaneously on several spacecraft. In these time intervals, we compute cross-correlation functions of spectral intensities summed over a frequency range. The frequency bandwidths over which we sum the spectral intensities are restricted to the frequency ranges in which the chorus elements were observed. In these bandwidths, the spectral intensity was ~2 orders higher than the intensity of the background noise. The spectral bandwidths in which the chorus elements occurred changed along the spacecraft orbits as is obvious from Figure 1. This is the same approach as that used by *Santolik and Gurnett* [2003] and *Santolik et al.* [2004a]. In this analysis, however, we admit time shifts between data from individual spacecraft, thus obtaining the cross-correlation function for each pair of spacecraft. We then searched for the time shifts at which the cross-correlation functions have maxima, and take these values of time shifts as representative. In the results that we are going to present, we used the Spearman cross-correlation functions applied to rank values [*Santolik et al.*, 2004a], since these are less sensitive to the interference by disturbing signals. The time shifts obtained from cross-correlation functions applied to measured intensities (Pearson cross correlation) are basically the same, but the cross-correlation coefficients are lower. It should also be noted that the time shifts obtained by the cross-correlation analysis of spectrograms containing several separated wave packets (elements) represent average time shifts observed between the corresponding elements in these selected time intervals. The time shifts measured between the elements separately exhibit some fluctuations.

[13] The characteristic frequencies and representative time shifts are displayed in Figures 5a and 5b as a function of time along the analyzed part of the orbit. The lines are again color coded according to the spacecraft in the same way as in Figures 3 and 4. Figures 5c and 5d show the characteristic frequency f normalized to the equatorial cyclotron frequency f_{ceq} calculated while using a dipole field model. We tried to estimate the accuracy of the dipole approximation of the magnetic field. For that purpose we calculated the equatorial cyclotron frequencies $f_{ceq(4.25)}$ at a fixed distance $L = 4.25$ while using the dipole field model and the measured cyclotron frequencies f_{ce} along the spacecraft orbits, $f_{ceq(4.25)} = fceq \cdot (L/4.25)^3$, where L is the L shell of the spacecraft. The *fceq* values are based both on the dipole approximation of the magnetic field and on the measured local electron cyclotron frequency f_{ce}. This correction therefore serves to check the validity of the dipole field model which only is a rough approximation of the real field because of the interaction of the Earth's magnetic field with the solar wind. If the dipole field model perfectly represented the actual magnetic field, then the dotted lines would be

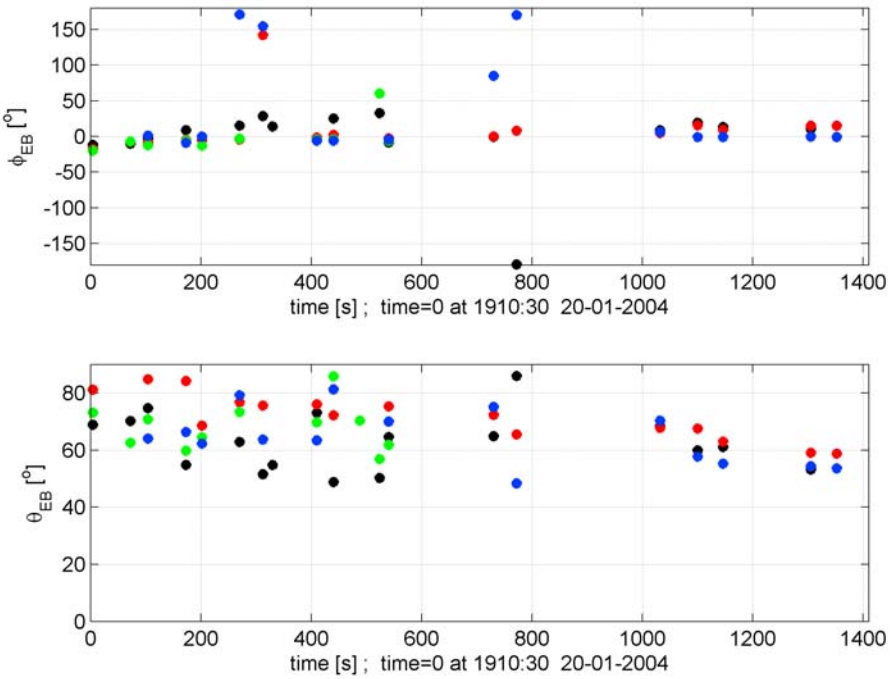

Figure 4. Wave normal angels computed by plane wave analysis from three magnetic and two electric field components measured by the STAFF instruments on different Cluster spacecraft, which are color coded as follows: SC1 is black, SC2 is red, SC3 is green, and SC4 is blue. Here θ is the polar angle and φ is the azimuthal angle, $\varphi = 0$ means that the wave vector points from the Earth.

constant and have a value of ~9.55 kHz measured at the equator at $L \sim 4.25$. The calculated $f_{ceq(4.25)}$ values are indicated by dotted lines in Figure 3d. We can see that the calculated values match the measured value of ~9.55 kHz close to the equator, approximately at *mlat* < 5°. At larger magnetic latitudes, the calculated values are higher, and roughly follow the measured values of the local f_{ce}. For example, at *mlat* ~ 15° the calculated $f_{ceq(4.25)} \sim 10.5$ kHz, which is approximately 1.1 times greater than the measured value.

[14] Returning to Figure 5 we can see that both the characteristic frequencies f observed and the normalized frequencies f/f_{ceq}' decrease with magnetic latitude. We used a correction $f/f_{ceq}' = (f/f_{ceq}) \cdot (f_{ceq(4.25)}/9.55)$ when displaying the normalized frequencies in Figure 5. We stress, however, that we consider the $f_{ceq(4.25)}/9.55$ values rather to be a test of the validity of the dipole field approximation, than a reliable correction factor. Without this correction, the decrease of normalized frequencies f/f_{ceq} would be even steeper, and their values at *mlat* ~ 15° would be ~10% lower. Note that if the waves propagated exactly along the magnetic field lines, then the normalized frequencies would remain constant with changing magnetic latitude, provided that the chorus is generated at the same normalized frequencies at the equator for different radial distances. *Santolik et al.* [2005b] showed that the ratio f/f_{ceq} is approximately constant in a wide range of radial distances. Note in Figure 5 that the radial distances changed from ~4.7 to ~4.2 during the analyzed time interval. We consider that the relatively steep decrease of f/f_{ceq} that we observed with increasing magnetic latitude could not be explained by the dependence of f/f_{ceq} on the radial distance of the source from the Earth; more probably it is a consequence of generation and propagation of the waves with high wave normal angles and group velocities oblique to the magnetic field lines. Note that high oblique angles were also obtained by the plane wave analysis presented in section 2.

[15] Special attention needs to be given to Figure 5d. Here we display the normalized frequencies f/f_{ceq} as a function of magnetic latitude, and not as a function of time. It is interesting to note that if different spacecraft pass the same magnetic latitude (owing also to the orbit about the same L shell), then they receive the same characteristic frequency during the analyzed time interval. This indicates that the conditions for chorus generation remained approximately constant during the analyzed time interval.

[16] We can estimate the angle β between the magnetic field and the group velocity from the dependence of f/f_{ceq} on *mlat*. First, we assume that chorus waves are generated with the same normalized frequency $f/fceq = 0.45$ at different radial distances at the equator. Next, we take a measured value $f_M/fceq$ outside, but not far from the equator, e.g., $f_M/fceq_2 = 0.4$ at the magnetic latitude $\lambda_M = 4.2°$ and $L_2 = 4.3$, where the dipole magnetic field is still a reasonable approximation. Since the normalized frequency at the equator had to be 0.45, the waves were originally generated at a higher L shell L_3, controlled by the equatorial cyclotron frequency $fceq_3$. In other words, we require that $f_M/fceq_3 = 0.45$. Using a dipole field model, we obtain

$$fceq_2/fceq_3 = 0.45/0.4 = (L_3/L_2)^3.$$

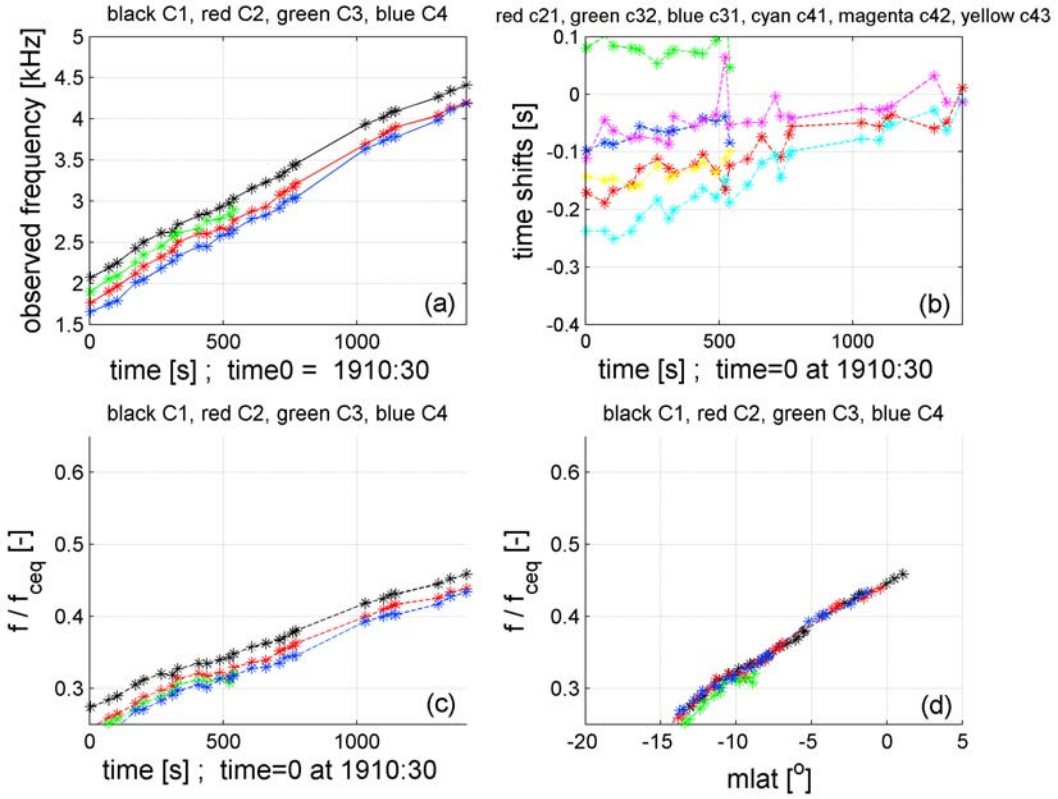

Figure 5. (a) Characteristic frequencies of the observed lower band chorus, and (b) time shifts between the corresponding elements observed on different spacecraft as functions of time. Positive values of the time shift t_{ij} (where i, j are numbers of the Cluster spacecraft) mean that the spacecraft i receives the corresponding element later than spacecraft j, i.e, the time shift $t_{ij} = t_i - t_j$. The time shifts are color coded as follows: red is t21, green is t32, blue is t31, cyan is t41, magenta is t42, and yellow is t43. (c) Observed characteristic frequencies f normalized to equatorial electron cyclotron frequency $fceq$ as functions of time, and (d) normalized frequencies $f/fceq$ as functions of the magnetic latitude during the analyzed time interval.

Thus, $L_3 = L_2 \cdot (0.45/0.4)^{1/3} = 4.3 \cdot (0.45/0.4)^{1/3} = 4.472$. Then, the angle β can be estimated from the geometry as follows:

$$\mathrm{tg}\beta = (L_2 - L_3)/(L_3 \cdot \lambda_M \cdot \pi/180).$$

The calculation gives $\beta = -27°$. Having used the full dispersion relation for cold plasmas [e.g., *Stix*, 1992] and the values measured at the equator ($f = 4.3$ kHz, $f_{ce} = 9.55$ kHz, and plasma frequency $f_p = 25$ kHz), we numerically found that $\beta = 27°$ corresponds to $\theta \sim 60°$. It should be noted that the plasma frequency (density) measurement by the WHISPER instrument was unreliable during the analyzed time interval (P. Decreau, private communication, 2007), however, comparisons with other similar orbits indicate that this value of plasma frequency should be reasonable. Note also that $\theta \sim 60°$ is in good agreement with the values obtained by wave normal analysis based on the STAFF measurements presented in Figure 4.

[17] Figures 6a and 6b present the time shifts between the corresponding elements and frequency differences between different spacecraft as a function of perpendicular distances of the spacecraft. We use equation (1) to calculate the perpendicular distance $d_{\perp ij}$ between the spacecraft i and j

$$d_{\perp ij} = |\mathbf{r_i} - \mathbf{r_j}| \cdot |\sin\varphi|, \qquad \cos\varphi = \frac{(\mathbf{r_i} - \mathbf{r_j}) \cdot \mathbf{B}}{|\mathbf{r_i} - \mathbf{r_j}| \cdot |\mathbf{B}|}, \qquad (1)$$

where **B** is the averaged magnetic field vector measured by the four Cluster spacecraft and $\mathbf{r_i}$ and $\mathbf{r_j}$ are the coordinate vectors of the spacecraft. We note that the perpendicular distances decreased as the spacecraft approached the equator (not shown), whereas the parallel distances increased at the same time, but insignificantly.

[18] From Figure 6, it is obvious that the time shifts and frequency differences increase almost linearly with the perpendicular distances between observation points (spacecraft). Figure 6c shows that the sign of the time shifts depends on the sign of the differences of L shells of the spacecraft locations. Note that the absolute values of the time shifts are basically the same for the same distances regardless of whether these are given as the difference of L shells at the equatorial plane or as the perpendicular distance in an arbitrary direction. In other words, the separation of the spacecraft in the radial

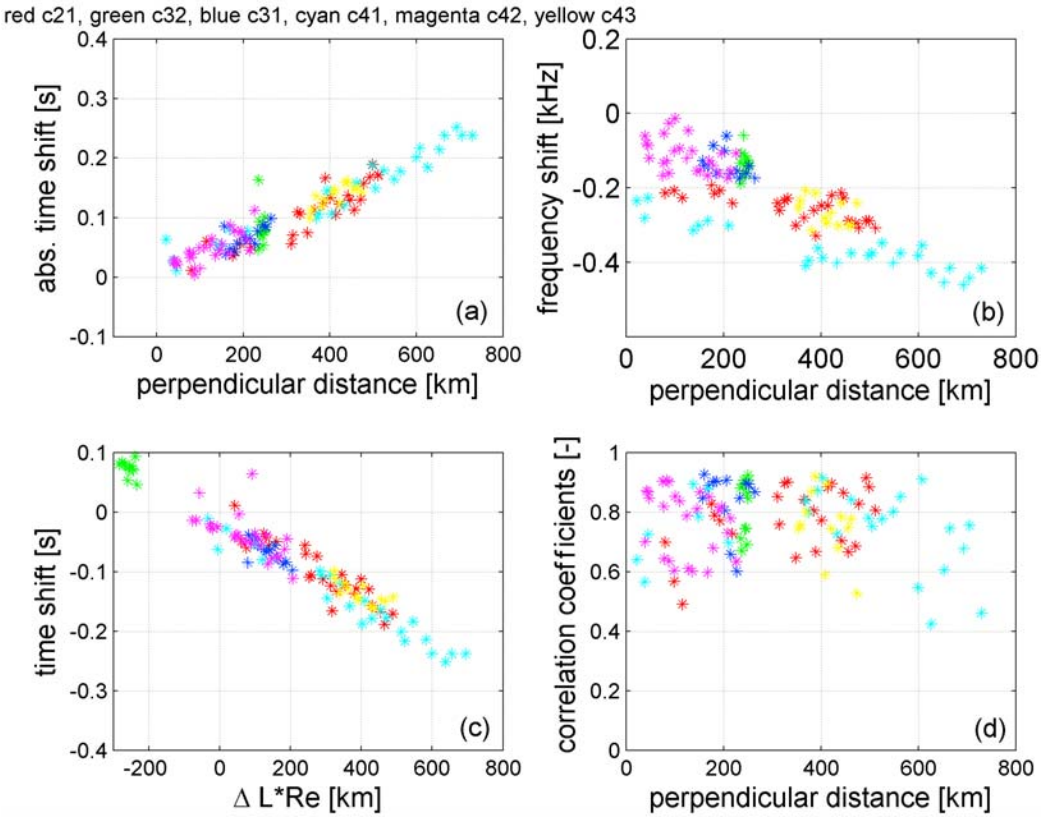

Figure 6. (a) Absolute value of time shifts as functions of the perpendicular distances of the spacecraft, and (c) time shifts as functions of differences of L shells of the spacecraft locations. Positive values of a time shift t_{ij} (where i, j are numbers of the Cluster spacecraft) mean that the spacecraft i receives the corresponding element later than spacecraft j, $t_{ij} = t_i - t_j$. The time shifts are color coded as follows: red is t21, green is t32, blue is t31, cyan is t41, magenta is t42, and yellow is t43. (b) Frequency differences, and (d) cross-correlation coefficients as functions of perpendicular distances of the spacecraft.

direction plays a critical role for the observed value of the time shift in this case. Figure 6d displays the rank cross-correlation coefficients. It shows that the spectrograms are significantly correlated at perpendicular distances up to ~500–600 km. These distances are much larger than those reported by *Santolik and Gurnett* [2003] in the case of storm time chorus. We point out that the large distances at which the spectrograms are correlated in our case, however, do not mean that chorus sources are so wide. If a source was 500–600 km wide, we would observe corresponding elements on all the spacecraft almost simultaneously, but we observe significant time shifts. Therefore, it is likely that chorus sources are much narrower than 500 km, probably less than 100 km as reported by *Santolik and Gurnett* [2003]. Possible chorus source properties leading to the presented phenomenon are based on the fact that we observed oblique waves, and this is discussed in section 4.

4. Hypotheses on Chorus Source Characteristics

[19] In this section, we will discuss three hypotheses suggesting chorus source properties that could result in the observed time shifts and frequency differences between the corresponding elements observed on different spacecraft. The first two hypotheses listed below were already published; therefore, we will mention them only briefly. We describe in more detail the third hypothesis, which is newly introduced and which is most consistent with the observed data.

[20] 1. The hypothesis proposed by *Inan et al.* [2004] and elaborated by *Platino et al.* [2006]. According to this hypothesis, frequency differences and time shifts between corresponding elements could be explained in terms of differential Doppler shifts and group velocities caused by a source which radiates in wide ranges of wave normal angles and moves rapidly along magnetic field lines. This approach attributes the whole frequency shift to the differential Doppler shift induced by the source motion and by the different values of the parallel component of the wave vector of waves propagating with different initial wave normal angles θ. It does not take into account the possibility that the different frequency ranges of one element are observed on different spacecraft because they propagate along different trajectories. The source locations found by *Platino et al.* [2006] were in several cases inconsistent with measured locations of the chorus source region. The Poynting flux measurements [e.g., *LeDocq et al.*, 1998; *Santolik et al.*, 2005b] showed that the region of the chorus source has a typical scale not larger than ~6000 km along the field line. Assuming the symmetry of the source with respect to the geomagnetic equatorial

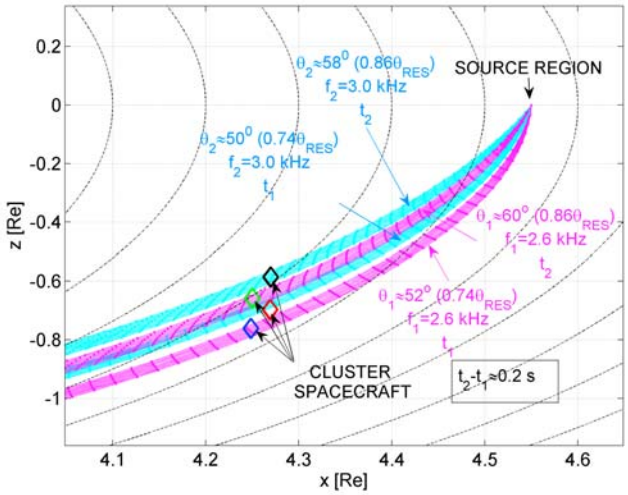

Figure 7. Simulated trajectories of 2.6 kHz waves (magenta) and 3.0 kHz waves (cyan) propagating from the geomagnetic equator for two different initial wave normal angles at two different times t_1 and t_2. Note that waves having higher frequency and higher initial wave normal angle propagate to the lower L shells. The locations of spacecraft correspond to 1919:30 UT on 20 January 2004.

plane, the source should not be located further than ∼3000 km from the equator, which corresponds to a magnetic latitude ∼6° at L = 4.5. However, *Platino et al.* [2006], using this hypothesis, located a chorus source to much larger distances from the equator, to magnetic latitudes up to ∼20°, from where the source emitted waves toward the equator (Figure 9 from *Platino et al.* [2006]).

[21] 2. An explanation proposed by *Chum et al.* [2007] based on the idea that a quasi-stationary source radiates in such a way that both frequency and wave normal angle change with the time. In this hypothesis, the trajectories of the waves change with time and the source subsequently irradiates different locations (spacecraft) in space. The principle is schematically presented in Figure 7 showing the ray trajectories obtained by ray tracing simulations for waves started at the geomagnetic equator with different initial conditions. Note that the ray trajectories depend on the frequency and wave normal angle θ. If the frequency and wave normal angle θ increase with time, then the waves propagate to lower L shells than they propagated to previously, and successively irradiate different spacecraft. The locations of spacecraft correspond to 1919:30 UT. The radial distance of the source in Figure 7 was chosen with regard to the correspondence between the simulated and measured values of wave normal angles θ by the STAFF instruments.

[22] 3. According to the third hypothesis, the observed time shifts and frequency differences between corresponding elements on different spacecraft result from sources moving across the field lines, toward the Earth in this case. As the source moves toward the Earth during the generation of a single element, the characteristic frequency of the emission increases owing to an increase of the electron cyclotron frequency, and consequently the spacecraft located at the lower L shells receive the corresponding element (a higher-frequency part of the element) later than the spacecraft located at higher L shells.

[23] An open question remains as to what could cause a transverse motion of the source. Since the measured time shifts reach a value of ∼0.2 s for the perpendicular distances of ∼560 km recalculated to the equatorial plane (Figure 5c), the transverse speed of the source motion should be ∼2800 km/s in this case. Considering a measured strength of the magnetic field (∼340 nT), it seems unlikely that the transverse motion could be caused by the $\boldsymbol{E} \times \boldsymbol{B}$ drift because this mechanism would require an unrealistically high azimuthal quasi-electrostatic field of ∼1V/m.

[24] It is interesting to investigate whether such a motion of the chorus source (instability region) could result from a wave-particle interaction. Let us assume that a feedback takes place between the waves and counter streaming electrons in the source region owing to electron cyclotron resonance. We assume that a weak, "seed" population of waves can be strongly and coherently amplified by counter streaming electrons that have been influenced by previously generated waves if the whole system is close to instability. Note that a feedback is supposed in the current theories attempting to explain the discrete character of chorus emissions [*Trakhtengerts*, 1995, 1999; *Trakhtengerts et al.*, 2007]. *Omura and Summers* [2006] showed that a nonlinear wave-particle interaction leads to the bunching of a part of the resonating electrons in the phase space. The bunched electrons in turn could cause instability and generation of successive waves. These theories and computer simulations [*Nunn et al.*, 1997; *Katoh and Omura*, 2006, 2007; *Omura et al.*, 2008], assume generation of chorus waves in the parallel direction with respect to the magnetic field for simplicity. If the oblique waves are generated, they encounter counter-streaming electrons on other field lines than those on which their generation was started. Consequently, if the feedback plays a role in the chorus generation, then the information shared between the particles and waves necessarily propagates across the magnetic field lines. Next, we try to estimate the velocity v_T of such a transverse motion.

[25] The wave particle interaction depends on the phase of the wave amplitude. We assume that for the coherent generation and for particles being in resonance with waves inside the generation region, the propagation of the phase of the wave field has to be taken into account. The wave phase is seen by a particle along the flow of the wave energy, i.e., along the ray trajectory. Therefore, we introduce the velocity $\boldsymbol{v_w}$ which is the phase velocity $\boldsymbol{v_f}$ projected into the direction of the group velocity $\boldsymbol{v_g}$. That means $\boldsymbol{v_w}$ is defined as the scalar product of $\boldsymbol{v_f}$ and $\boldsymbol{v_g}$ divided by the absolute value of $\boldsymbol{v_g}$

$$v_{w\|} = \frac{v_{f\|} \cdot v_{g\|}}{\sqrt{v_{g\|}^2 + v_{g\perp}^2}} = \frac{\omega \cdot k_{\|} \cdot v_{g\|}}{\left(k_{\|}^2 + k_{\perp}^2\right) \cdot \sqrt{v_{g\|}^2 + v_{g\perp}^2}}, \tag{2}$$

$$v_{w\perp} = \frac{v_{f\perp} \cdot v_{g\perp}}{\sqrt{v_{g\|}^2 + v_{g\perp}^2}} = \frac{\omega \cdot k_{\perp} \cdot v_{g\perp}}{\left(k_{\|}^2 + k_{\perp}^2\right) \cdot \sqrt{v_{g\|}^2 + v_{g\perp}^2}}. \tag{3}$$

A schematic picture clarifying the estimation of the velocity v_T is presented in Figure 8. For simplicity, we assume that the

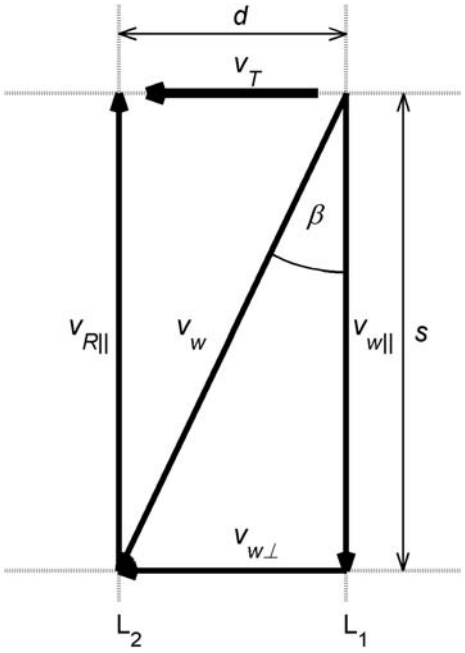

Figure 8. A schematic picture showing the velocities used in the estimation of the transverse velocity v_T of the source. Used symbols are as follows: v_w is the phase velocity of chorus waves projected into the group velocity, $v_{R||}$ is the parallel component of the velocity of resonating electrons, and β is the angle between the magnetic field and group velocity.

velocity of chorus propagation and parallel velocities of resonating electrons do not change substantially in the generation region. We consider that an oblique wave propagates a short phase path s along the field line and a short phase path d perpendicular to the field line, respectively, during a short time interval t_{s1}. Consequently, the counter streaming electrons influenced by this wave and moving with the velocity $v_{R||}$ reach the same magnetic latitude (e.g., magnetic equator) after having traveled the distance s in the time interval t_{s2}. Between these quantities, the following relations hold: $v_T = d/t_s$, $t_s = t_{s1} + t_{s2}$, $t_{s1} = d/v_{w\perp} = s/v_{w||}$, $t_{s2} = s/v_{R||}$.

[26] After rearranging we get

$$v_T = \frac{v_{w\perp} \cdot v_{R||}}{(v_{w||} + v_{R||})}. \quad (4)$$

In general, the wave growth can continuously occur anywhere inside the length s that approximately determines the chorus source length along the field line. However, we assume that on average, the largest wave growth occurs very close to the equator and we do not assume any longitudinal drift of the source region for simplicity.

[27] Obviously, the phase and group velocities and hence also the velocity v_T depend on the normalized frequency f/f_{ceq}, plasma frequency f_p, and wave normal angle θ through the dispersion relation. The parallel velocity of the electrons $v_{R||}$ is obtained from the resonance condition. We consider the first-order cyclotron resonance. Figure 9 shows the calculated transverse velocity v_T as a function of wave normal angle θ for the values measured at the equator, i.e., f = 4.3 kHz, f_{ceq} = 9.55 kHz and two different values of plasma frequency, f_p = 25 kHz and f_p = 30 kHz (see section 3 with regard to the value used for f_p). Note that for small values of θ, i.e., chorus generated parallel or antiparallel to the magnetic field lines, the transverse velocity is relatively low. However, the transverse velocity v_T strongly increases for angles θ larger than the value of the Gendrin angle [*Gendrin*, 1961] owing to the increase of the parallel component of the group and phase velocities. For angles approaching the resonance cone, v_T decreases again because of the decrease of the phase and group velocities to zero and because of the decrease of the parallel velocity of resonating electrons.

[28] The estimated velocity $v_T \sim$ 2800 km/s from the cross-correlation analysis is of the same order as the calculated values of v_T. The maximum of the calculated v_T reaches a value about two times higher than the estimated value of $v_T \sim$ 2800 km/s. The calculated values of v_T for $\theta \sim 60^\circ$ are relatively close to the estimated velocity $v_T \sim$ 2800 km/s. Note that $\theta \sim 60^\circ$ was both measured by STAFF at the equator and estimated from the f/f_{ceq} dependence on magnetic latitude. However, the exact comparison is impossible. First, the dependence of v_T on the angle θ is very steep at these values; thus, a small inaccuracy in θ measured leads to large difference in v_T. Second, if the chorus waves are generated with a span of wave normal angles, an effective value of v_T should be taken. The calculation of the effective value of v_T is however impossible without the knowledge of the wave power distribution for various angles and the knowledge of the mechanism of the wave particle interaction.

[29] The definition of v_w (2) and (3) as the phase velocity projected onto the group velocity may be a questionable point. It could also be reasonable to define v_w as the group velocity projected onto the phase velocity (wave vector direction); equations (2) and (3) would then only differ in the denominator. It would also be possible to define v_w

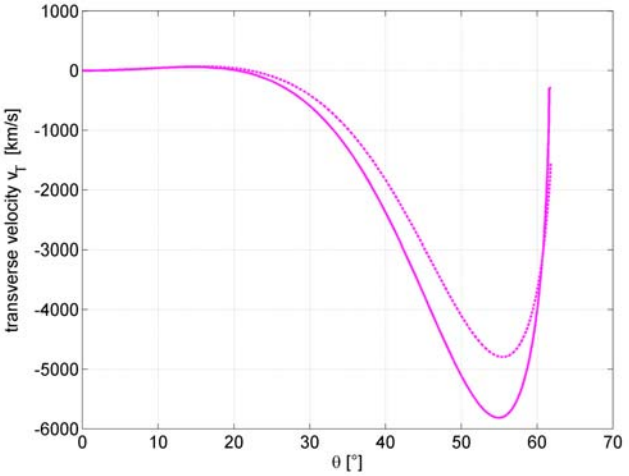

Figure 9. Computed transverse velocity v_T as a function of wave normal angle θ for electrons resonating at the equator at Re = 4.25 with waves of a frequency 4.3 kHz for f_{ceq} = 9.55 kHz and plasma frequency f_p = 25 kHz (solid line) and f_p = 30 kHz (dashed line).

simply as the group velocity. The curves in Figure 9 would then have similar shapes ($v_T = 0$ at $\theta = 0$, $\theta = \theta_G$ and v_T approaching zero at the resonance cone), but the absolute values would be ~1.4 times larger at the angles of interest in the analyzed case. We justify our definition of v_w by the requirement that the wave field that is effective in the amplification process has to stay in resonance with the counter streaming electrons along the flow of wave energy in the source, and by the fact that our definition of v_w gives results that match better the observations.

[30] We have also analyzed a similar relatively short event recorded on 6 January 2004. We have also observed falling tones during this event (not shown). Similarly to the case recorded on 20 January, the spacecraft located at lower L shells received a corresponding chorus element later than the spacecraft located on higher L shell, regardless of the relative distance from the equator. The measured (observed) transverse velocity was ~2000 km/s. The normalized frequency *f/fceq* at the equator was again 0.45, while the measured values of plasma frequency and electron cyclotron frequency at the equator were ~30 kHz and 8.45 kHz, respectively. The calculated values of the transverse velocity v_T were a bit lower than in the case presented in Figure 9, with the maximum value of 4200 km/s.

[31] We consider that equation (4) represents an upper limit for the transverse velocity v_T because the feedback between the waves and counter streaming electrons may not be continuous or equally efficient all the time during the generation of a chorus element. We remind that the feedback is the cause for the transverse motion of the generation region.

[32] The fact that the cross-correlation coefficients (Figure 6) fluctuate and do not exhibit a systematic dependence on perpendicular distance might be a consequence of the time variation of the power intensity emitted by the chorus source during its transverse motion.

4.1. Comparing the Hypotheses Explaining the Time Shifts and Frequency Differences With the Observed and Analyzed Data

[33] We have discussed three different chorus source properties that could theoretically lead to the observed time shifts and frequency differences. It is difficult to uniquely determine which mechanism is responsible for the observed differences. We cannot exclude the possibility that the frequency differences and time shifts are caused by the net effect of the hypotheses described. However, we have already mentioned that the application of the first hypothesis can locate the source to relatively high magnetic latitudes, which is inconsistent with the measured Poynting flux locations of the chorus sources. Moreover, the systematic linear dependence of the time shifts and frequency differences on the perpendicular distance between the spacecraft could hardly be explained by the differential group velocities and differential Doppler shifts of waves generated by a rapidly moving source. For the latter reason (the linear dependence of the time shifts and frequency differences on the perpendicular distance) we think that it is also not likely that the second mechanism dominates, though it naturally explains the steeply falling elements [*Chum et al.*, 2007].

[34] We stress that both the first and second hypotheses require that the different spacecraft receive waves that are generated and propagating at different wave normal angles with respect to the magnetic field. This is, however, not the case as demonstrated in Figure 4 where the measured wave normal angles are all about the same value.

[35] The third mechanism (a generation region moving across the L shells) is in agreement with the values of measured wave normal angles. Moreover, the transverse motion of the source naturally explains the linear dependence of the time shifts observed on the perpendicular distance of the spacecraft in the radial direction. It is also consistent with the idea that a feedback exists between waves and particles in the process of the generation of discrete chorus emissions. As we discussed earlier, it is reasonable to expect that this feedback results in the transverse motion of the source generating oblique waves. We have not investigated, however, the physical process involved in this feedback. An introduction to the nonlinear interaction between energetic electrons and coherent oblique whistler waves was given by *Bell* [1984]. The third mechanism is also consistent with the fact that different spacecraft receive the same characteristic frequencies when approaching the same L shell and magnetic latitude. We therefore consider that the transverse motion of the source is the major reason for the time shifts and frequency differences observed.

[36] We also stress that we did not use the ray tracing simulation to estimate the velocity v_T of the chorus source transverse motion caused by the feedback between the obliquely propagating waves and resonating electrons. Note that the ray tracing simulation was only used in the case of hypothesis II. The estimate of the transverse velocity is based on the observations and measurements performed very close to the generation region and/or in it. As it is obvious from equations (2)–(4), the transverse velocity v_T is a function of plasma density since the group velocity and the velocity of resonating electrons depend on it. Worth noticing is that a significant transverse motion occurs whenever the waves are generated with wave normal angles between the Gendrin angle θ_G and the resonance cone. If the waves are generated at $\theta = 0$ or $\theta = \theta_G$ then $v_T = 0$ since the perpendicular component of the group velocity is zero. We point out again that the calculated v_T is in good agreement with the observation for the measured $\theta \sim 60^\circ$ and a realistic range of plasma densities. In turn, the estimated wave distribution function for this case presented by *Santolik et al.* [2009] shows that chorus is generated in a relatively narrow range of polar angles θ, $\Delta\theta \sim 2^\circ$–$3^\circ$, while the span in azimuthal angle is relatively large (see Figure 4e of *Santolik et al.* [2009]).

4.2. Comparing the Analysed Case With Other Observations of Oblique Chorus

[37] Although many measurements performed close to the chorus source region indicate that chorus is generated with the wave normal angles corresponding to quasi-parallel (antiparallel) propagation with respect to the magnetic field [e.g., *Hayakawa et al.*, 1984; *LeDocq et al.*, 1998; *Santolik et al.*, 2003], several ray tracing studies have shown that chorus can also be generated with oblique angles [*Lauben et al.*, 2002; *Chum et al.*, 2003]. *Lauben et al.* [2002] were the first who concluded that lower band chorus is generated with wave normal angles close to the Gendrin angle. They used ray tracing simulations with initial values of wave normal angles obtained by multicomponent measurements

on the POLAR spacecraft. Later on, *Chum and Santolik* [2005], *Santolik et al.* [2006], and *Bortnik et al.* [2007] showed that, without the presence of ducts, only chorus generated with oblique angles, usually close to the Gendrin angle with wave vector directed downward, can propagate far away from the magnetic equator, reach high latitudes and possibly convert to plasmaspheric hiss.

[38] The presented observation and analysis is, however, different in several respects. First, we infer that chorus was generated at wave normal angles larger than Gendrin angle θ_G, which was $\sim 20^\circ$ in this case (f = 4.3 kHz and f_{ceq} = 9.55 kHz). The observed angles ($\theta \sim 60^\circ$) were relatively close to the resonance cone [*Santolik et al.*, 2009]. Note that the θ_G can be identified in Figure 9 as the angle at which $v_T = 0$, which is a consequence of the perpendicular component of the group velocity being zero for waves propagating at $\theta = \theta_G$ besides the case $\theta = 0$. The resonance cone corresponds to the rightmost end of the curve representing v_T in Figure 9.

[39] Secondly, the presented analysis is based on the observations of frequency and time shifts between corresponding elements on several Cluster spacecraft. As we mentioned in sections 1 and 4, such observations were already reported by several authors [e.g., *Gurnett et al.*, 2001; *Inan et al.*, 2004; *Platino et al.*, 2006; *Chum et al.*, 2007; *Breneman et al.*, 2007, 2009]. This observation is however unique in that we observed significant time shifts between lower band chorus elements at frequencies below 4 kHz with simultaneous multicomponent measurements by the STAFF instruments, which makes the determination of wave normal angles possible. Note that at least one of the following possibilities occurred in other published cases while none of them invalidates the analysis of the presented case: (1) the corresponding elements were not observed, owing to large mutual distances between the spacecraft [e.g., *Santolik et al.*, 2004b]; (2) the corresponding elements were observed without detectable time shifts [e.g., *Santolik et al.*, 2003]; and (3) the time shifts between the corresponding elements were observed above 4 kHz [*Inan et al.*, 2004; *Platino et al.*, 2006; *Chum et al.*, 2007], which is the upper frequency limit of the multicomponent measurement by STAFF.

[40] The only similar observation which we know of is the already mentioned observation on 6 January 2004 leading to similar results. That observation was done, however, over a shorter time interval of $\sim$4 minutes.

[41] Because of the uniqueness of this observation it is difficult to state how frequent the frequency-time shifts of chorus elements generated at such highly oblique angles are. However, we believe that, in general, all observations reporting the time and frequency shifts between corresponding elements are related to chorus generation at oblique angles. Note that oblique propagation is a common feature in these reports, regardless of the hypothesis proposed and the absolute values of θ estimated. A comprehensive statistical wave normal analysis of a large number of chorus events is necessary to resolve this problem. That is, however, beyond the scope of this paper. Nevertheless, we consider that the presented case study is important since it clearly shows that the oblique propagation may lead to phenomena that we do not encounter in the case of quasi-parallel propagation. We also conclude that the generation at oblique angles needs to be taken into account in future theoretical studies and simulation to quantify correctly the influence of chorus waves on the electron radiation belt dynamics.

5. Summary

[42] We presented a systematic observation of significant time shifts and frequency differences between the corresponding elements of the lower band chorus observed by the WBD instruments on different Cluster spacecraft on 20 January 2004.

[43] The cross-correlation analysis showed that the time shifts and frequency differences between corresponding chorus elements depend almost linearly on the perpendicular (radial) distances between the spacecraft. The spacecraft located at lower L shells observed the corresponding elements later than the spacecraft located at higher L shells, regardless of the fact that they were located further from the magnetic equatorial plane, where the Poynting flux analysis based on the STAFF measurements located the chorus sources.

[44] The spectrograms are significantly correlated at perpendicular distances up to $\sim$500–600 km. The significant time shifts observed, however, indicate that the chorus sources are much narrower, probably having the transverse dimension less than $\sim$100 km as was reported by *Santolik and Gurnett* [2003].

[45] The normalized frequencies *f*/*fceq* strongly decreased with increasing magnetic latitude. This dependence of *f*/*fceq* on the magnetic latitude is stable during the analyzed time interval, and results from the propagation of the chorus waves at highly oblique angles. The highly oblique angles are also obtained by the wave normal analysis based on the multicomponent measurements by the STAFF instruments [*Santolik et al.*, 2009].

[46] We consider that chorus sources moving transverse to magnetic field lines to lower L shells could for the most part explain the time shifts and frequency differences observed. The transverse motion of the source could result from a feedback between the waves generated at oblique angles and counter streaming electrons. We provided an expression for the velocity of the transverse motion of the chorus source. The transverse velocity gains relatively large values if the chorus waves are generated at wave normal angles between the Gendrin angle and resonance cone. We cannot exclude the possibility that mechanism II and/or I described in section 4 also contribute to the time shifts and frequency differences observed, thus diminishing the role of the transverse motion and velocity, respectively.

[47] **Acknowledgments.** We thank N. Cornilleau-Wehrlin from CETP, IPSL, Velizy, France for the data from the STAFF instrument. We would like to acknowledge grant 205/09/1253 of the Grant Agency of the Czech Republic, grant A301120601 of the Grant Agency of the Academy of Sciences of the Czech Republic, and grant RITA-CT-2006-025969 of LAPBIAT 2. The research at the University of Iowa was supported by NASA Goddard Space Flight Center under grant NNX07AI24G.

[48] Amitava Bhattacharjee thanks the reviewers for their assistance in evaluating this paper.

References

Bell, T. F. (1984), The nonlinear gyroresonance interaction between energetic electrons and coherent VLF waves propagating at an arbitrary angle

with respect to the Earth's magnetic field, *J. Geophys. Res.*, *89*(A2), 905–918, doi:10.1029/JA089iA02p00905.

Bortnik, J., R. M. Thorne, and N. P. Meredith (2007), Modeling the propagation characteristics of chorus using CRRES suprathermal electron fluxes, *J. Geophys. Res.*, *112*, A08204, doi:10.1029/2006JA012237.

Breneman, A., C. A. Kletzing, J. Chum, O. Santolik, D. Gurnett, and J. Pickett (2007), Multispacecraft observations of chorus dispersion and source location, *J. Geophys. Res.*, *112*, A05221, doi:10.1029/2006JA012058.

Breneman, A. W., C. A. Kletzing, J. Pickett, J. Chum, and O. Santolik (2009), Statistics of multispacecraft observations of chorus dispersion and source location, *J. Geophys. Res.*, *114*, A06202, doi:10.1029/2008JA013549.

Burtis, W. J., and R. A. Helliwell (1976), Magnetospheric chorus: Occurrence patterens and normalized frequency, *Planet. Space Sci.*, *24*, 1007–1024, doi:10.1016/0032-0633(76)90119-7.

Chum, J., and O. Santolik (2005), Propagation of whistler-mode chorus to low altitudes: Divergent ray trajectories and ground accessibility, *Ann. Geophys.*, *23*, 3727–3738.

Chum, J., F. Jiricek, J. Smilauer, and D. Shklyar (2003), Magion 5 observations of chorus-like emissions and their propagation features as inferred from ray-tracing simulation, *Ann. Geophys.*, *21*, 2293–2302.

Chum, J., O. Santolik, A. W. Breneman, C. A. Kletzing, D. A. Gurnett, and J. S. Pickett (2007), Chorus source properties that produce time shifts and frequency range differences observed on different Cluster spacecraft, *J. Geophys. Res.*, *112*, A06206, doi:10.1029/2006JA012061.

Cornilleau-Wehrlin, N., et al. (1997), The Cluster spatio-temporal analysis of field fluctuations (STAFF) experiment, *Space Sci. Rev.*, *79*, 107–136, doi:10.1023/A:1004979209565.

Gendrin, R. (1961), Le guidage des whistlers par le champ magnetique, *Planet. Space Sci.*, *5*, 274–282, doi:10.1016/0032-0633(61)90096-4.

Gurnett, D., and F. Scarf (1981), Determination of Jupiter's electron density profile from plasma wave observations, *J. Geophys. Res.*, *86*(A10), 8199–8212, doi:10.1029/JA086iA10p08199.

Gurnett, D. A., R. L. Huff, and D. L. Kirchner (1997), The wide-band plasma wave investigation, *Space Sci. Rev.*, *79*, 195–208, doi:10.1023/A:1004966823678.

Gurnett, D. A., R. L. Huff, J. S. Pickett, A. M. Persoon, C. A. Kletzing, R. L. Mutel, I. W. Christopher, U. S. Inan, W. L. Martin, and J. L. Bougeret (2001), First results from the Cluster wideband plasma wave investigation, *Ann. Geophys.*, *19*, 1259–1272.

Hayakawa, M., Y. Yamanaka, M. Parrot, and F. Lefeuvre (1984), The wave normals of magnetospheric chorus emissions observed on board GEOS 2, *J. Geophys. Res.*, *89*, 2811–2821, doi:10.1029/JA089iA05p02811.

Horne, R. B., and R. M. Thorne (2003), Relativistic electron acceleration and precipitation during resonant interactions with whistler mode chorus, *Geophys. Res. Lett.*, *30*(10), 1527, doi:10.1029/2003GL016973.

Horne, R. B., R. M. Thorne, S. A. Glauert, J. M. Albert, N. P. Meredith, and R. R. Anderson (2005), Timescale for radiation belt electron acceleration by whistler mode chorus waves, *J. Geophys. Res.*, *110*, A03225, doi:10.1029/2004JA010811.

Inan, U. S., M. Platino, T. F. Bell, D. A. Gurnett, and J. S. Pickett (2004), Cluster measurements of rapidly moving sources of ELF/VLF chorus, *J. Geophys. Res.*, *109*, A05214, doi:10.1029/2003JA010289.

Katoh, Y., and Y. Omura (2006), A study of generation mechanism of VLF triggered emission by self-consistent particle code, *J. Geophys. Res.*, *111*, A12207, doi:10.1029/2006JA011704.

Katoh, Y., and Y. Omura (2007), Computer simulation of chorus wave generation in the Earth's inner magnetosphere, *Geophys. Res. Lett.*, *34*, L03102, doi:10.1029/2006GL028594.

Lauben, D. S., U. S. Inan, T. F. Bell, and D. A. Gurnett (2002), Source characteristics of ELF/VLF chorus, *J. Geophys. Res.*, *107*(A12), 1429, doi:10.1029/2000JA003019.

LeDocq, M. J., D. A. Gurnett, and G. B. Hospodarsky (1998), Chorus source locations from VLF Poynting flux measurements with the Polar spacecraft, *Geophys. Res. Lett.*, *25*(21), 4063–4066, doi:10.1029/1998GL900071.

Menietti, J. D., R. B. Horne, D. A. Gurnett, G. B. Hospodarsky, C. W. Piker, and J. B. Groene (2008), A survey of Galileo plasma wave instrument observations of Jovian whistler-mode chorus, *Ann. Geophys.*, *26*, 1819–1828.

Nunn, D., Y. Omura, H. Matsumoto, I. Nagano, and S. Yagitani (1997), The numerical simulation of VLF chorus and discrete emissions observed on the Geotail satellite using a Vlasov code, *J. Geophys. Res.*, *102*(A12), 27,083–27,097, doi:10.1029/97JA02518.

Omura, Y., and D. Summers (2006), Dynamics of high-energy electrons interacting with whistler mode chorus emissions in the magnetosphere, *J. Geophys. Res.*, *111*, A09222, doi:10.1029/2006JA011600.

Omura, Y., D. Nunn, H. Matsumoto, and M. J. Ryccroft (1991), A review of observational, theoretical and numerical studies of VLF triggered emissions, *J. Atmos. Sol. Terr. Phys.*, *53*, 351–368, doi:10.1016/0021-9169(91)90031-2.

Omura, Y., Y. Katoh, and D. Summers (2008), Theory and simulation of the generation of whistler-mode chorus, *J. Geophys. Res.*, *113*, A04223, doi:10.1029/2007JA012622.

Platino, M., U. S. Inan, T. F. Bell, J. S. Pickett, and P. Canu (2006), Rapidly moving sources of upper-band ELF/VLF chorus near the magnetic equator, *J. Geophys. Res.*, *111*, A09218, doi:10.1029/2005JA011468.

Reinleitner, L., W. Kurth, and D. A. Gurnett (1984), Chorus-related electrostatic bursts at Jupiter and Saturn, *J. Geophys. Res.*, *89*(A1), 75–83, doi:10.1029/JA089iA01p00075.

Santolik, O., and D. A. Gurnett (2003), Transverse dimensions of chorus in the source region, *Geophys. Res. Lett.*, *30*(2), 1031, doi:10.1029/2002GL016178.

Santolik, O., M. Parrot, and F. Lefeuvre (2003), Singular value decomposition methods for wave propagation analysis, *Radio Sci.*, *38*(1), 1010, doi:10.1029/2000RS002523.

Santolik, O., D. A. Gurnett, and J. S. Pickett (2004a), Multipoint investigation of the source region of storm-time chorus, *Ann. Geophys.*, *22*, 2555–2563.

Santolik, O., D. A. Gurnett, J. S. Pickett, M. Parrot, and N. Cornilleau-Wehrlin (2004b), A microscopic and nanoscopic view of storm-time chorus on 31 March 2001, *Geophys. Res. Lett.*, *31*, L02801, doi:10.1029/2003GL018757.

Santolik, O., D. A. Gurnett, J. S. Pickett, M. Parrot, and N. Cornilleau-Wehrlin (2005a), Central position of the source region of storm-time chorus, *Planet. Space Sci.*, *53*, 299–305, doi:10.1016/j.pss.2004.09.056.

Santolik, O., E. Macusova, K. H. Yearby, N. Cornilleau-Wehrlin, and H. SC. K. Alleyne (2005b), Radial variation of whistler-mode chorus: First results from the STAFF/DWP instrument onboard the Double Star TC 1 spacecraft, *Ann. Geophys.*, *23*, 2937–2942.

Santolik, O., J. Chum, M. Parrot, D. A. Gurnett, J. S. Pickett, and N. Cornilleau-Wehrlin (2006), Propagation of whistler-mode chorus to low altitudes: Spacecraft observations of structured ELF hiss, *J. Geophys. Res.*, *111*, A10208, doi:10.1029/2005JA011462.

Santolik, O., D. A. Gurnett, J. S. Pickett, J. Chum, and N. Cornilleau-Wehrlin (2009), Oblique propagation of whistler mode chorus/hiss in its source region, *J. Geophys. Res.*, *114*, A00F03, doi:10.1029/2009JA014586.

Sazhin, S. S., and M. Hayakawa (1992), Magnetospheric chorus emissions: A review, *Planet. Space Sci.*, *40*, 681–697, doi:10.1016/0032-0633(92)90009-D.

Stix, T. H. (1992), *Waves in Plasmas*, Am. Inst. of Phys, New York.

Trakhtengerts, V. Y. (1995), Magnetosphere cyclotron maser: Backward wave oscillator generation regime, *J. Geophys. Res.*, *100*, 17,205–17,210, doi:10.1029/95JA00843.

Trakhtengerts, V. Y. (1999), A generation mechanism for chorus emission, *Ann. Geophys.*, *17*, 95–100, doi:10.1007/s005850050739.

Trakhtengerts, V. Y., A. G. Demekhov, E. E. Titova, B. V. Kozelov, O. Santolik, E. Macusova, D. Gurnett, J. S. Pickett, M. J. Rycroft, and D. Nunn (2007), Formation of VLF chorus frequency spectrum: Cluster data and comparison with the backward wave oscillator model, *Geophys. Res. Lett.*, *34*, L02104, doi:10.1029/2006GL027953.

J. Chum, Department of Upper Atmosphere, Institute of Atmospheric Physics, Bocni II 1401, 141 31 Prague 4, Czech Republic. (jachu@ufa.cas.cz)

D. A. Gurnett and J. S. Pickett, Department of Physics and Astronomy, University of Iowa, Iowa City, IA 52242-1479, USA. (donald-gurnett@uiowa.edu; pickett@uiowa.edu)

O. Santolik, Faculty of Mathematics and Physics, Charles University, Ke Karlovu 3, 121 16 Prague 2, Czech Republic. (ondrej.santolik@mff.cuni.cz)